Effects of counterion size on the attraction between similarly charged surfaces

Jasna Zelko,[1] Aleš Iglič,[2] Veronika Kralj-Iglič,[1] and P. B. Sunil Kumar[3,a)]

[1]*Laboratory of Clinical Biophysics, Faculty of Medicine, University of Ljubljana, Ljubljana, Slovenia*
[2]*Laboratory of Biophysics, Faculty of Electrical Engineering, University of Ljubljana, Ljubljana, Slovenia*
[3]*Department of Physics, Indian Institute of Technology Madras, Chennai, India*

Interaction between similarly charged surfaces can be attractive at high electrostatic coupling constants $\Xi = l_B Z^2/\mu_{GC}$, where l_B is the Bjerrum length, μ_{GC} the Gouy–Chapman length, and Z the valency of counterions. While this effect has been studied previously in detail, as a function of surface charge density and valency of the pointlike counterions, much less is known about the effect of counterion size. We apply the Wang–Landau sampling Monte Carlo (MC) simulation method to compute the free energy F as a function of the scaled distance between the plates $\widetilde{D} = D/\mu_{GC}$ for a range of Ξ and scaled counterion radii $\widetilde{R} = R/\mu_{GC}$. We find that for large Ξ and small ion radius, there is a global equilibrium distance $\widetilde{D} = \widetilde{D}_{eq} = 2(1 + \widetilde{R})$, correctly giving the expected value at the point counterion limit. With increasing $\widetilde{R}$ the global minimum in $F(\widetilde{D})$ changes to a metastable state and finally this minimum vanishes when $\widetilde{R}$ reaches a critical value, which depends on Ξ. We present a state diagram indicating approximate boundaries between these three regimes. The Wang–Landau MC method, as it is applied here, offers a possibility to study a wide spectrum of extended problems, which cannot be treated by the use of contact value theorem. © *2010 American Institute of Physics*. [doi:10.1063/1.3506896]

I. INTRODUCTION

Interaction between charged bodies is one of the oldest problems studied in physics. The fact that it remains an active area of research even today indicates the complexity of this problem and its importance in a wide variety of areas.[1] It has been shown that valency, charge distribution, and size of the ions can play a major role in determination of the nature of this interaction, leading to nontrivial effects like attraction between like-charged surfaces and repulsion between oppositely charged surfaces.[2–4] Also, the present work draws motivation from experimental observation of attractive interaction between two charged phospholipid membranes of giant unilamellar vesicles when oppositely charged proteins or antibodies were present in the solution.[5,6] Till recently most of the theoretical models of the ion mediated interaction between charged surfaces focused on the role of point counterions (CIs) in mediating the attractive interaction between two charged plates. Strong coupling theories have been successful in explaining the attraction between similarly charged surfaces mediated by pointlike counterions at high coupling constants.[7] Properties of an electrical double layer of one charged plate and an electrolyte solution with point ions have also been extensively studied theoretically and by simulations.[8,9]

One of the dominant view points on ion specificity is that it is determined by the solvation factor.[10] Recently there has been some effort to understand the effect that finite ion size has on the electrostatic interactions. It is believed that size of the ions is one major factor leading to ion specificity observed in biological systems, e.g., selective ion transport in charged pores.[11,12] Though systematic investigations on the effect of finite ion size were not carried out, it was recognized quite early that they play an important role in the interaction between two similarly charged plates.[13–16] The importance of finite ion size in the electric double layer calculations was also looked into in Refs. 17–23. A recent study of this problem took into account only the finite size effects of condensed counterions and plate charges, assuming them to be in the same plane.[24]

In the past Monte Carlo (MC) simulations have been carried out in parallel with the theoretical calculations for point counterions confined between two similarly charged plates[7] as well as for counterions of finite size (primitive model).[14,15] These simulations were limited to calculation of the density distribution of the counterions between the plates, from which electrostatic potential and pressure profile between the plates were determined using the contact value theorem.[25,26] The study reported here differs from that carried out in the past on two aspects: (a) we determined the free energy of the system as a function of distance between plates using the Wang–Landau (WL) sampling scheme[27,28] and (b) we carry out a systematic investigation of the interaction between plates as a function of the counterion size. From the free energy we can compute the pressure profile as a function of distance between plates. The method used is validated by comparing the results obtained in the limit of point counterions,[7] in the limit of hard sphere fluid,[29] and those obtained from contact value theorem for counterions of finite size.[14] In all cases our simulations show good agreement with previous simulations and theory for hard sphere fluid.

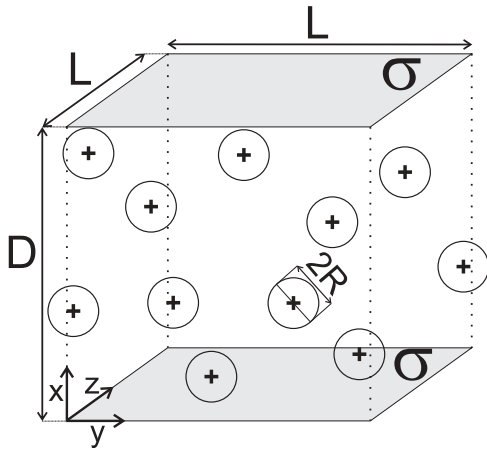a)Author to whom correspondence should be addressed. Electronic mail: sunil@physics.iitm.ac.in.

FIG. 1. Schematic presentation of simulation model. Hard spherical counterions with centered charges between two similarly charged hard walls.

II. MODEL

We consider two equally charged impermeable plates with surface charge density σ, extending in the yz plane. The plates are separated in the x direction for a distance D (Fig. 1). Periodic boundary conditions are employed along the yz plane and hard boundary conditions along the x direction. The medium in between the plates is considered to be a dielectric continuum with a permittivity $\varepsilon = 80$. CIs are modeled as hard spheres of radius R with a charge of valency Z at its center. Surface charge density of the plates σ and valency Z of the CIs are of opposite sign. The strength of the interaction between plates is determined by the size R of the CIs and the electrostatic coupling constant:

$$\Xi = \frac{2\pi Z^3 l_B^2 \sigma}{e_0}, \tag{1}$$

where $l_B = e_0^2/(4\pi\varepsilon\varepsilon_0 k_B T)$ is the Bjerrum length.[7] All distances are rescaled in terms of the Gouy–Chapman length:

$$\mu_{\rm GC} = \frac{e_0}{(2\pi l_B Z \sigma)}. \tag{2}$$

Rescaled distances are marked with tilde: $\widetilde{x} = x/\mu_{\rm GC}$. The lateral dimension of the simulation box $\widetilde{L} = L/\mu_{\rm GC}$ and the number of CIs, N, are related through the electroneutrality condition: $\widetilde{L} = \sqrt{\pi N \Xi}$. In the simulations reported in this article we set $N = 100$ for charged particles and $N = 300$ for the uncharged ones.

The maximum value of $\widetilde{R}$ is chosen in the simulations such that at the minimum separation between plates $\widetilde{D} = 2\widetilde{R}$ the ions can be accommodated in a single layer. At the same time, the fraction of volume occupied by the counterions is always below the freezing transition for hard spheres.[30]

Total electrostatic energy of the system is composed of the contributions from counterion–counterion interactions, counterion–plate interactions, and plate–plate interaction. Finite size of the ions is taken into account through hard-core interactions between the counterions themselves and between plates and counterions. To compute electrostatic interaction energy between plates, $E_{\sigma\sigma}$, we take the energy per unit area

for two infinite plates with a continuous charge density σ on them and multiply it by the area of the plates to get

$$E_{\sigma\sigma} = \frac{-\sigma^2 L^2 D}{(2\varepsilon\varepsilon_0)}. \tag{3}$$

Similarly, electrostatic energy of interaction between counterions and the two plates $E_{Z\sigma}$ is

$$E_{Z\sigma} = \frac{-\sigma N Z e_0 D}{(2\varepsilon\varepsilon_0)}. \tag{4}$$

$E_{\sigma\sigma}$ and $E_{Z\sigma}$ depend only on the distance between the plates and not on the particle positions. The counterion–counterion interactions are calculated using periodic boundary conditions in the y and z directions.[7] The total electrostatic contribution due to counterion–counterion interactions E_{ZZ} is

$$E_{ZZ} = \frac{Z^2 e_0^2}{4\pi\varepsilon\varepsilon_0} \sum_{i,j>i} \sum_{\mathbf{n}} \frac{1}{|\mathbf{r}_i - \mathbf{r}_j + \mathbf{n}|}, \tag{5}$$

where $\mathbf{r}_i$ and $\mathbf{r}_j$ refer to counterion positions. To carry out the sum over the periodic images $\mathbf{n}$, we use the method developed by Lekner[31] by writing the sum in Eq. (5) as

$$\sum_{\mathbf{n}} \frac{1}{|\mathbf{r}_i - \mathbf{r}_j + \mathbf{n}|} = A - \ln(\cosh(2\pi\Delta x) - \cos(2\pi\Delta y))$$

$$+ 4 \sum_{p=1}^{P} \cos(2\pi p\Delta z) \sum_{m=-M}^{M} K_0$$

$$\times (2\pi p \sqrt{(\Delta y + m)^2 + \Delta x^2}), \tag{6}$$

where we have used the dimensionless quantities defined as: $\Delta x = |x_i - x_j|/L$, $\Delta y = |y_i - y_j|/L$, $\Delta z = |z_i - z_j|/L$. $|y_i - y_j|$, and $|z_i - z_j|$ are the minimum image distance between two particles along the y and z direction, respectively. A is a constant that depends on the reference state and K_0 is the Bessel function. For values of $\rho = \sqrt{(\xi + m)^2 + \Delta x^2} < 1/3$ (where ξ is the smaller among Δy and Δz), we replace the sum of Bessel functions with the Sperb formula[32]

$$4 \sum_{p=1}^{P} \cos(2\pi p\Delta z) K_0 (2\pi p \rho)$$

$$= -1.386\,294 + 2\ln(\rho)$$

$$+ \frac{1}{\sqrt{\Delta z^2 + \rho^2}} - \Psi(1 + \Delta z) - \Psi(1 - \Delta z)$$

$$+ \sum_{s=1}^{S} \binom{-\frac{1}{2}}{s} \rho^{2s} [\zeta(2s+1, 1 + \Delta z)$$

$$+ \zeta(2s+1, 1 - \Delta z)]. \tag{7}$$

Here Ψ is the digamma function and ζ is the Hurwitz zeta function. This makes the calculation more accurate since the Bessel function diverges for small arguments. We found that using $P = 4$, $M = 2$, and $S = 3$ is sufficient to get numerically consistent results for coupling constants and distances presented in this paper.

III. SIMULATION DETAILS

In this paper the free energy F, as a function of the distance D between the plates, is evaluated using the Wang–Landau sampling scheme. The Wang–Landau algorithm was originally proposed for the calculation of density of states $\rho(E)$ and its usefulness was demonstrated explicitly for discrete phase space of the Ising model.[28] Soon the extensions of the original method followed, including sampling of two-dimensional density of states,[33,34] continuum (off-lattice) systems,[35] quantum systems,[36] and expanded ensembles.[37–39] The expanded ensemble is usually characterized by some reaction coordinate D, which groups states of a system to substates with different values of reaction coordinate. Each substate of the expanded ensemble is weighted by the probability density $g(D)$. In our simulations D corresponds to the distance between the plates.

In the original Wang–Landau method the density of states is initially set to unity for all points within a specified range of energy. A random walk is performed in energy space, within this specified interval. Transition probabilities between states are determined by the ratio of the density of these states. Every time a state is visited, the corresponding density of state is multiplied by a modification factor (larger than one) and the histogram of energies is updated by adding a constant factor to the corresponding histogram bin. The procedure is repeated till the histogram is flat, which is then reset to zero and the modification factor reduced to its square root. The iteration is repeated till the required accuracy (modification factor close to unity) is achieved. In the work presented here this idea is applied to expanded ensemble which includes the distance D between the plates as a reaction coordinate. We keep the sampling still to one dimension with the density of states now replaced by probability density $g(D)$ and instead of a histogram in energy space, a histogram of distances $H(D)$ is sampled. Different states are sampled using a Metropolis scheme with the Hamiltonian $E + \Phi(D)$, where $E = E_{\sigma\sigma} + E_{ZZ} + E_{Z\sigma}$, and $\Phi(D)$ is related to the probability density $g(D)$ and free energy $F(D)$ through

$$F(D) = -k_B T \ln g(D) = -k_B T \Phi(D). \tag{8}$$

In the simulations reported here, one Monte Carlo sweep (MCS) consists of N counterion moves and one plate move, where N is the number of CIs between the plates. Within one MCS, a particle move or a plate move is chosen randomly with probabilities $N/(N+1)$ and $1/(N+1)$, respectively.[40] When a CI is picked an attempt is made to move it to a new position within a predetermined box centered about it. This move is accepted with the standard Metropolis scheme. During a plate move the distance between plates is changed by $\delta\widetilde{D}$ from $\widetilde{D}_{old}$ to $\widetilde{D}_{new} = \widetilde{D}_{old} \pm \delta\widetilde{D}$. The value of $\delta\widetilde{D}$ is between 0.7 and 1.0. After each plate move the CIs' positions are rescaled to

$$\widetilde{x}_{new} = \widetilde{R} + (\widetilde{x}_{old} - \widetilde{R})(\widetilde{D}_{new} - 2\widetilde{R})/(\widetilde{D}_{old} - 2\widetilde{R}),$$
$$\widetilde{y}_{new} = \widetilde{y}, \quad \widetilde{z}_{new} = \widetilde{z}. \tag{9}$$

The transition probability for such moves is[35,41]

$$A_{(old\rightarrow new)} = N_D\, e^{-[(\Phi_{new} + E_{new}) - (\Phi_{old} + E_{old})]}. \tag{10}$$

The prefactor $N_D = \left[(\widetilde{D}_{new} - 2\widetilde{R})/(\widetilde{D}_{old} - 2\widetilde{R})\right]^N$ comes in because of the volume change of the system.[40] The important thing to note is that only the ratio of the volume available to the centers of hard spheres has to be taken into account. Any move that violates the hard-core condition between ions and that between an ion and a surface is rejected.

The separation between plates in a chosen interval $\widetilde{D}_{min}$ to $\widetilde{D}_{max}$ is binned to a certain number of discrete states. The values of $\Phi(\widetilde{D})$ and $H(\widetilde{D})$ are initially set to 0 for all values of $\widetilde{D}$ in the chosen interval. Each time the state corresponding to the distance $\widetilde{D}$ is visited, the value of $\Phi(\widetilde{D})$ is increased by a constant convergence factor f: $\Phi(\widetilde{D}) = \Phi(\widetilde{D}) + f$, and the histogram of distances is updated $H(\widetilde{D}) = H(\widetilde{D}) + 1$. The flatness of the histogram is checked each 1000 MCS and when $H(\widetilde{D})$ is regarded as "flat," the convergence factor is rescaled $f = f \times 0.5$ (initially $f = 0.5$ is taken), the histogram $H(\widetilde{D})$ is reset to zero, and the sampling is repeated. The flatness criteria require that for all possible $\widetilde{D}$ the histogram $H(\widetilde{D})$ is not less than 80% of the average histogram value $\langle H(\widetilde{D}) \rangle$. As the value of f approaches zero the function $\Phi(\widetilde{D})$ approaches the logarithm of the true probability density. The simulation proceeds until f reaches a certain low threshold value.

As observed by Kim *et al.*[37] in the case of sampling along a reaction coordinates, the convergence factor need not be as precise as when density of states is calculated. We found that $f < 10^{-4}$ is sufficiently small for good convergence of $\Phi(\widetilde{D})$, and good agreement with theoretical results and earlier simulations was obtained. As already proposed in the original paper of Wang and Landau,[28] the total range of values of $\widetilde{D}$ that we want to sample can be divided into smaller segments (we used segments spanning over a distance of 3 Gouy–Chapman lengths) and the simulations are run separately for each segment. The values of $\Phi(\widetilde{D})$ should be such that nearby segments overlap at least in three points. Different segments are then put together by matching values in the overlapping end regions. No attempt is made to relate probability density to a known reference state; therefore $\Phi(\widetilde{D})$ and $F(\widetilde{D})$ are only determined up to an additive constant. One should keep in mind that free energy as well as Lekner–Sperb electrostatic energy can only be determined up to a constant. For convenience we shift all the free energy curves such that they approach 0 at large $\widetilde{D}$.

IV. RESULT AND DISCUSSION

First the correctness of the method is checked for the case of point CIs. The standard practice in the field of electrical double layer simulations is to use Metropolis MC scheme to evaluate the density distribution of ions between the plates at a fixed distance, from which, with the use of contact value theorem,[1] the pressure normal to the plates can be extracted.

Hence to compare our results with results published earlier by others, we computed the rescaled normal pressure $\widetilde{P}_N = P_N e_0^2/(2\pi l_B \sigma^2)$, where
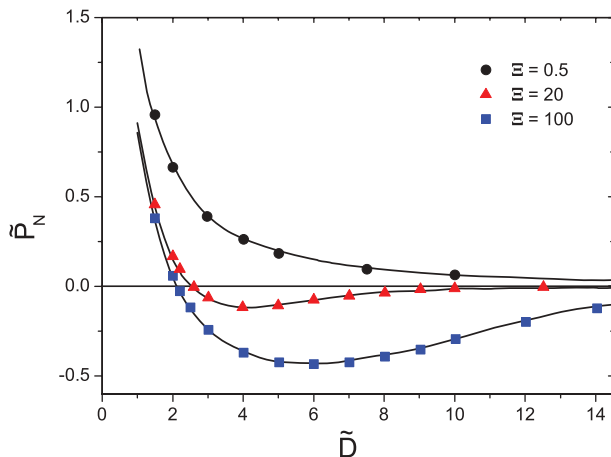
$$P_N = -L^{-2}\frac{dF}{dD} \tag{11}$$

FIG. 2. Rescaled pressure $\widetilde{P}_N = P_N \, e_0^2 / (2\pi l_b \sigma^2)$ as a function of rescaled distance $\widetilde{D}$ for different coupling constants. Smooth lines show the pressure obtained by differentiation of the free energy obtained by WL method. Points show data from Moreira and Netz (Ref. 7).

is the derivative of the unscaled free energy with respect to the unscaled distance between plates. As shown in Fig. 2 our results agree well with the results obtained by Moreira and Netz.[7]

Next we checked the applicability of the method to obtain the equation of state for a hard sphere fluid. Equation of state of the hard sphere fluid in a cubical geometry (all sides of equal length, i.e., $D = L$), with periodic boundary condition in all directions, is plotted in Fig. 3. The pressure P obtained by differentiating the Wang–Landau free energy F with respect to the volume and the theoretical results from Carnahan–Starling equation of state[29] are shown. Excellent agreement is found between the Carnahan–Starling theoretical prediction and our simulations.

In an earlier work, Valleau *et al.* had computed the normal pressure between two charged plates, with hard spherical counterions in between,[14] using contact value theorem that takes into account the finite size of ions.[25,26] In Fig. 4 we com-

FIG. 4. Normal pressure and free energy (inset) as a function of the space between plates $(D - 2R)$ available to the CIs. Surface charge density is $\sigma = -0.224 \text{ As/m}^2$, valency $Z = 2$, and ion radius $R = 3$ Å. The open squares are from Ref. 14.

pare the results obtained from our Wang–Landau approach with that from Ref. 14. The pressure is computed by using Eq. (11) where the free energy was obtained for the same parameters as used in Ref. 14. Note that, to make the comparison easy, here we plot the unscaled pressure. The data from these two approaches agree well.

Having convinced ourselves about the validity and applicability of the method, to compute the interaction between charged plates, we now compute $F(\widetilde{D})$ for different coupling constants and CI radii. For coupling constant $\Xi = 10$ (Fig. 5), where the interactions are repulsive over the whole range of values of D for pointlike CIs, increasing ion size only results in increasing the distance of closest approach between the plates. However, the behavior becomes more interesting for higher coupling constants (i.e., $\Xi \geq 20$) where, in the point ion limit, long range attraction is observed (Fig. 6). We are interested in the effect that the size of ions has on this attractive interaction. In order to explore this, we computed the free energy for coupling constants $\Xi = 20$ (not shown), $\Xi = 40$
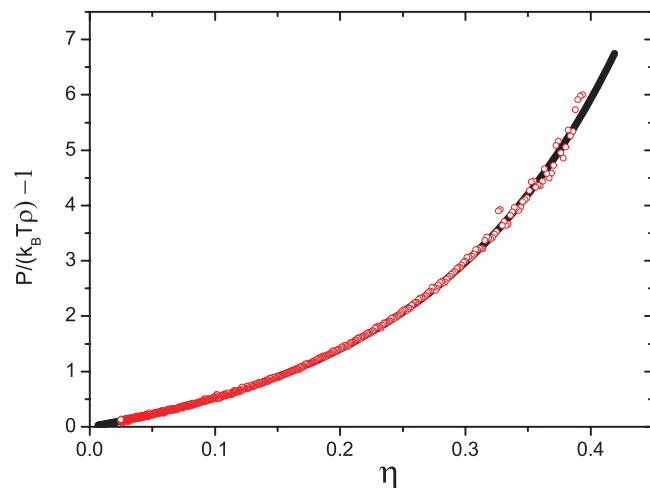

FIG. 3. Equation of states of hard spheres in a cubic box geometry, obtained from the Wang–Landau free energy (open circles) and with the Carnahan–Starling theory (continuous curve).
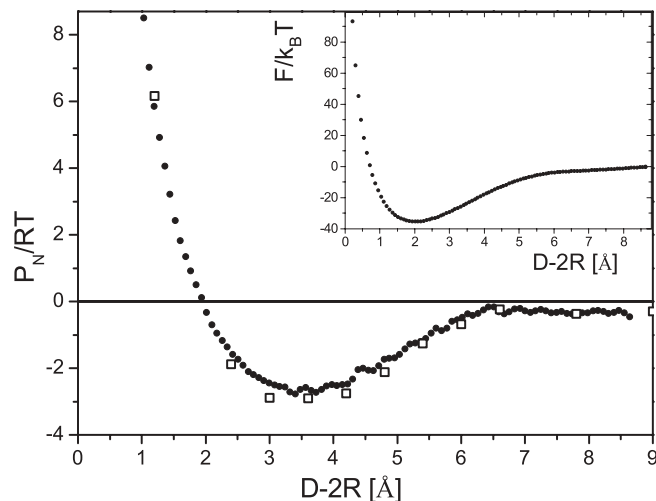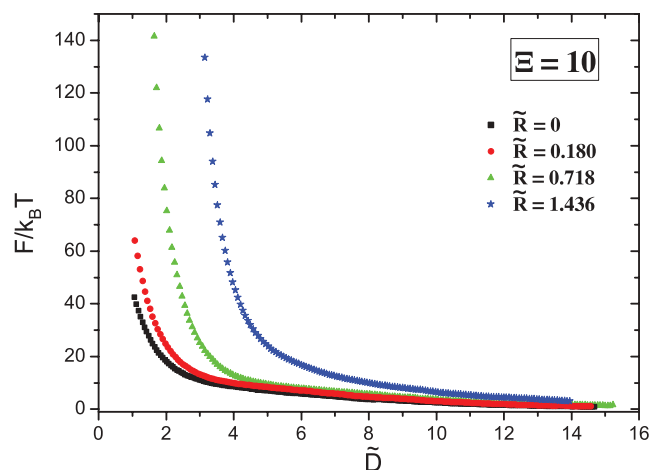

FIG. 5. Free energy as a function of the rescaled distance $\widetilde{D}$ for coupling constant $\Xi = 10$ and different ion radii $\widetilde{R}$.
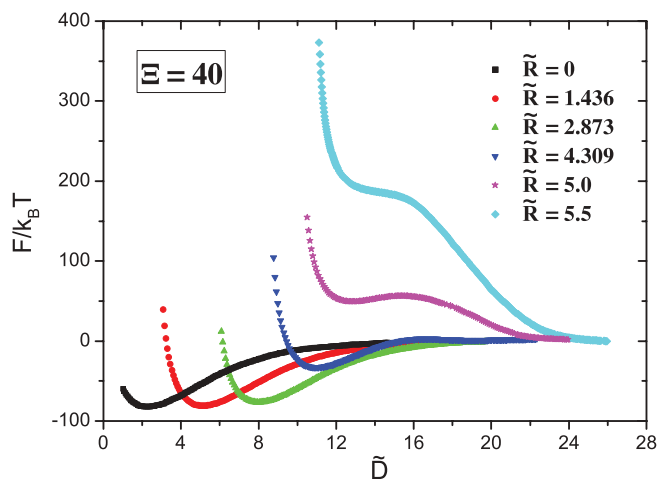
FIG. 6. Free energy as a function of the rescaled distance $\widetilde{D}$ for coupling constant $\Xi = 40$ and different ion radii $\widetilde{R}$.

FIG. 8. Free energy as a function of the rescaled effective separation $\widetilde{D} - 2\widetilde{R}$ for coupling constant $\Xi = 40$ and different ion radii $\widetilde{R}$.

(Fig. 6), $\Xi = 65$ (not shown), and $\Xi = 100$ (not shown). From these calculations, we see that there is a systematic shift in the free energy profile. The interaction between the plates changes from attractive to repulsive as $\widetilde{R}$ is increased and the value of $\widetilde{R}$ at which this happens increases with Ξ. We will explore this in greater detail below.

The dependence of free energy on the effective separation between plates $\widetilde{D} - 2\widetilde{R}$, for coupling constant $\Xi = 40$, is shown in Fig. 8. We see that for small enough $\widetilde{R}$ the free energy curves, shifted by $2\widetilde{R}$, coincide with the curve corresponding to point ions (e.g., see curves for $\widetilde{R} = 1.436$ and 2.873 in Fig. 8). If the ion size is increased beyond a certain value, which depends on Ξ, the depth of the minimum in the free energy starts to decrease and the interaction undergoes a change from attractive to repulsive regime. We show in Fig. 7 the normal pressure as a function of the distance between plates, where this can be clearly observed.

Plotting the pressure as a function of the size of the ions, for a given distance between plates, reveals another picture (see Fig. 10). In the region where attraction is still present, the pressure as a function of $\widetilde{R}$ first decreases and then in-
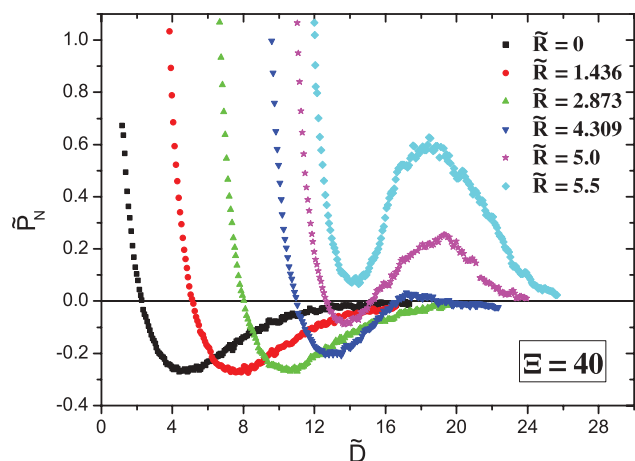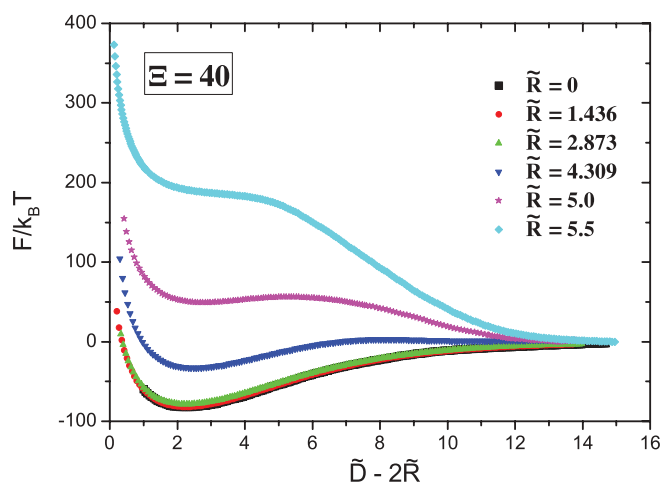
creases. The nonmonotonic behavior of the pressure in this region arises from the competition between the electrostatic and hard-sphere contributions. The contribution to the pressure from the total electrostatic interactions alone, for a given plate separation, is a decreasing function of the ion radius. This is a consequence of the fact that the electrostatic energy curves for different ionic radii fall on each other if plotted against $\widetilde{D} - 2\widetilde{R}$ (Fig. 13 left). On the other hand, the hard sphere contribution to the pressure, which for these plate separations is a monotonically increasing function of ion radius, is significant only when the scaled ion radius is larger than four[42] (Fig. 13 right). As can be seen from Fig. 10, this is indeed the range at which we have a minimum in the pressure indicating that beyond this size of ions, the negative pressure arising from the electrostatic interaction is overwhelmed by steric effects.

We show the equilibrium distance between the plates $\widetilde{D}_{eq}$ (the minimum in the free energy), as a function of the ion radius $\widetilde{R}$, in Fig. 11. For each coupling constant, $\widetilde{D}_{eq}$ is a linear function of $\widetilde{R}$. Again, deviations from this linear behavior are observed just before the minimum disappears for large $\widetilde{R}$.
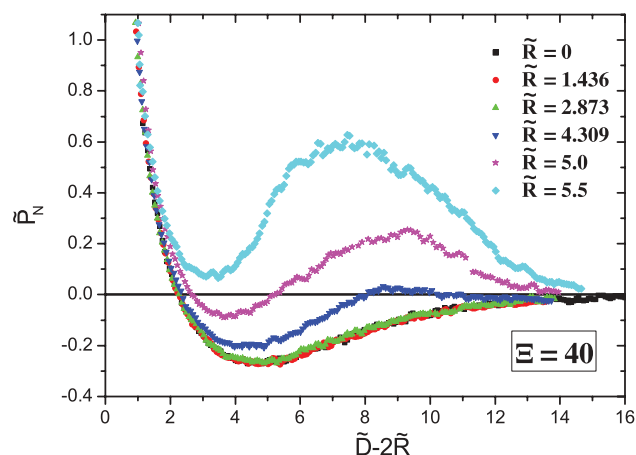

FIG. 7. Pressure as a function of the rescaled distance $\widetilde{D}$ for coupling constant $\Xi = 40$ and different ion radii $\widetilde{R}$.

FIG. 9. Pressure as a function of the rescaled effective separation $\widetilde{D} - 2\widetilde{R}$ for coupling constant $\Xi = 40$ and different ion radii $\widetilde{R}$.
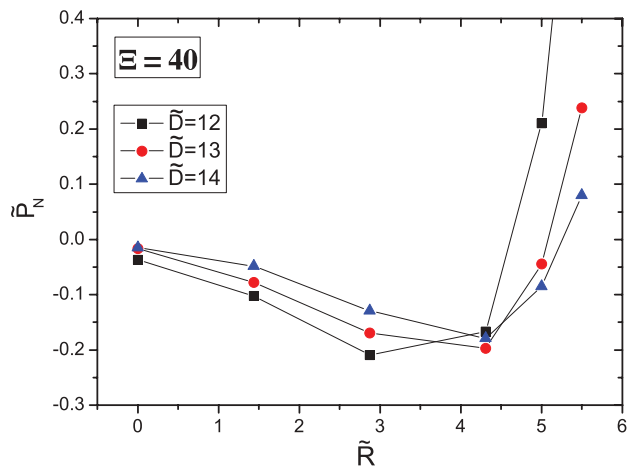
FIG. 10. The rescaled pressure as a function of the rescaled ion size for three different distances between the plates.

In the limit of point ions (i.e., $\tilde{R} = 0$) the value of $\tilde{D}_{eq}$ approaches the value 2 as the coupling constant is increased, which is also the prediction of strong coupling theory.[43] At the same time, the slope also approaches 2 with increasing coupling constant (Fig. 11). This essentially means that for small ion radii the effect of the ion size is only to shift the free energy minima by $2\tilde{R}$. The positions of the first minimum in free energy can thus approximately be predicted for intermediate coupling constants, e.g., $20 \leq \Xi \leq 65$. Though we did not check it explicitly, we expect the dependence of $\tilde{D}_{eq}$ on $\tilde{R}$ for higher coupling constants $\Xi > 65$ to be similar to that for $\Xi = 65$. However, when the ion radius is large enough, the first minimum in free energy disappears and repulsive regime is observed over the whole range of $\tilde{D}$, as is the case for $\tilde{R} = 5.5$ in Fig. 6. This is seen even better in Fig. 7, where we show that for $\tilde{R} = 5.5$ the normal pressure remains positive, which means that no attraction is present for these parameters.

Looking at the free energy, which is shifted by an arbitrary factor to match zero value at large distances between plates, we observe four different regimes of interaction,

depending on the size of the ions and the coupling constant. (A) For sufficiently small $\tilde{R}$, the minimum value of the free energy remains constant while its position, compared to that for point ions, is shifted by $2\tilde{R}$ to the right. (B) By increasing the radius of ions, the depth of the minimum starts to decrease but its position follows the same relation as described in (A). (C) In the third regime the minimum of $F(\tilde{D})$ is followed by a maximum, as can be seen for $\tilde{R} = 5.0$ in Fig. 8. The position of the minima is no longer obtained by shifting that for point ions by $2\tilde{R}$. (D) In the fourth regime the free energy is a monotonically decreasing function of the distance between plates, as is seen for $\tilde{R} = 5.5$ in Fig. 8.

Since the electrostatic interaction depends only on the coupling constant Ξ and the steric interaction is characterized by the finite ion size $\tilde{R}$, a parameter which can qualitatively characterize the interaction between the plates is the ratio of the two-dimensional volume fraction $\eta_2 = N\pi R^2/L^2$ and the square root of the coupling constant $\sqrt{\Xi}$. We name this quantity the interaction parameter: $ip = \eta_2/\sqrt{\Xi}$. In the strong coupling theory $\sqrt{\Xi}$ is connected to the lateral distance between the point ions $\tilde{a}_\perp \sim \sqrt{\Xi}$.[43] The interaction regimes, described in the previous paragraph, can be roughly determined with the use of the parameter ip, as is shown in Fig. 12. The data obtained from simulations are marked as points, where different symbols correspond to different regimes from A to D described above. Dashed straight lines are drawn to indicate approximate boundary between different regimes.

As pointed out earlier[13] the ionic radius affects electrostatic, entropic, and steric terms via the distribution of ions. However, we observe that for the parameters used in our simulations, the electrostatic energy contribution to the free energy (F_E) is much less influenced by the ion size than the rest of the terms ($F_H = F - F_E$). The total electrostatic energy of the system, with CIs having radius $\tilde{R}$, can thus be overlapped with that for point ions if plotted against $\tilde{D} - 2\tilde{R}$ (Fig. 13 left). Small deviations from this curve are observed only for the largest ion sizes. Or in other words, as far as the electrostatic energy is concerned, the effect of the hard-core interaction between the ions is mainly to decrease the
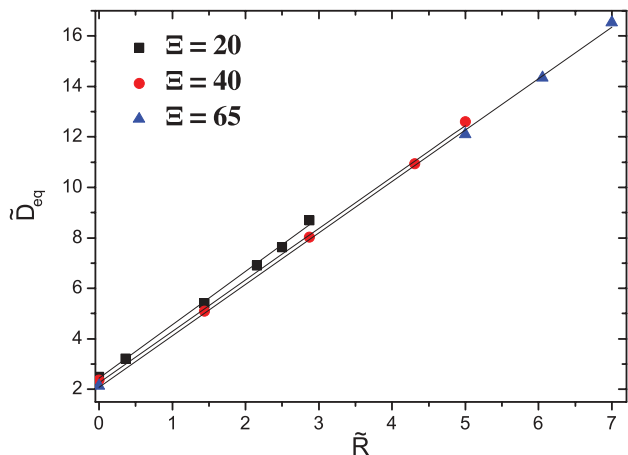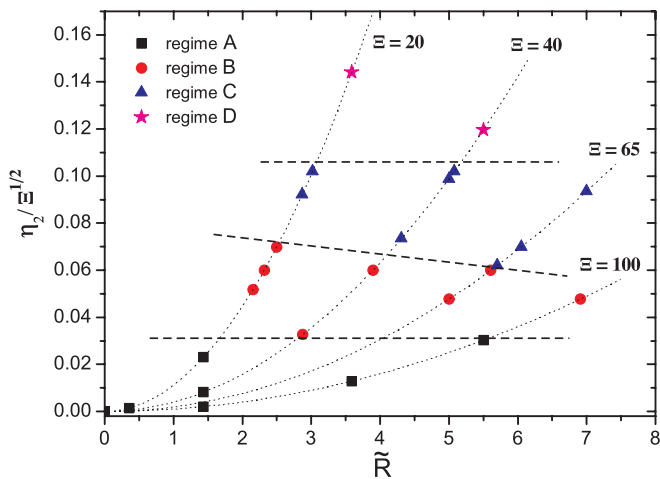

FIG. 11. Positions of the first minimum in free energy as a function of the rescaled radius of ions for different coupling constants together with a linear fit for each coupling constant.

FIG. 12. Rough state diagram of the different regimes of interaction as a function of "interaction" parameter $\eta_2/\sqrt{\Xi}$ and ion radius. Dashed lines denote approximate boundaries between regimes: A, B, C, and D. Dotted lines are only to indicate data points for a given value of Ξ.
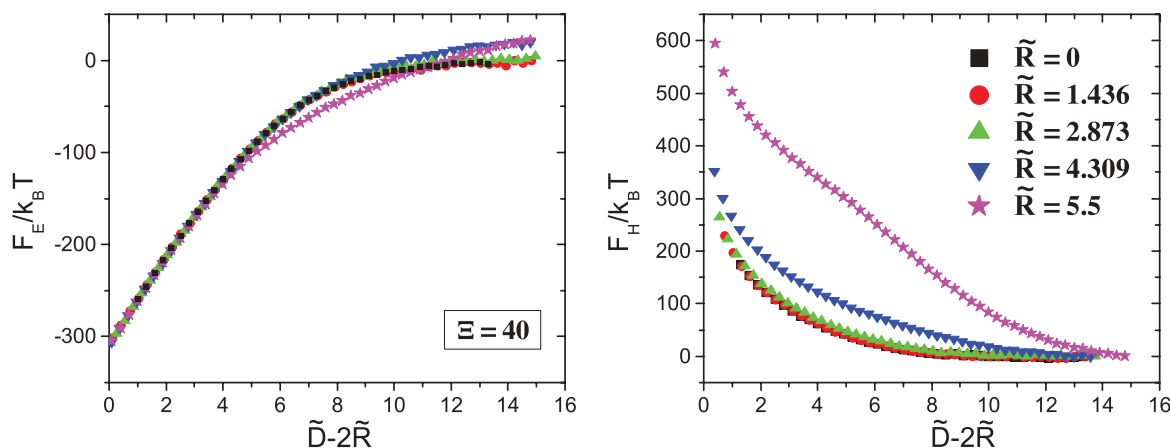
FIG. 13. Total electrostatic energy F_E (left) and entropic+steric contribution obtained by subtracting F_E from the free energy F (right), for the coupling constant $\Xi = 40$ and different ion radii.

effective separation between the double layers by $2\widetilde{R}$. On the other hand, rest of the free energy depends much more strongly on the ion size due to the steric interactions between ions. This is shown in Fig. 13 (right) where F_H plotted against $\widetilde{D} - 2\widetilde{R}$ shows clear deviation from the curves for point counterions even for moderate size of the ions. However, as already recognized by others, the steric interactions are negligible as long as the ion size is much smaller than the average lateral separation between ions and therefore for very small values of the ion radius we see F_H overlapping with the curve for point ions when plotted against $\widetilde{D} - 2\widetilde{R}$.

This implies that, for small CI diameters where the steric effects are negligible, the free energy and pressure curves overlap with curves for point CIs when shifted by $2\widetilde{R}$ (see Figs. 8 and 9). On increasing the CI radius, the free energy and pressure curves, even though shifted by $2\widetilde{R}$, start to deviate from that of point ions. The amount of deviation from the point CI curve is identified by regimes B–D described above. Hence we conclude that these deviations (transitions from regimes A to D) are mainly driven by steric effects, which are most dominant for $2\widetilde{R} + 2 < \widetilde{D} < 4\widetilde{R} + 2$. From Fig. 9 we can clearly see that independent of the CI size $\widetilde{R}$, the pressure curves are identical for $\widetilde{D} - 2\widetilde{R} < 2$ and $\widetilde{D} > 4\widetilde{R} + 2$, which supports the above argument. For large ion radii the steric effects dominate and the free energy curves are similar to that for neutral hard sphere fluids in similar confining geometries. At intermediate size of the ions, the barrier in the free energy curves appears when $\widetilde{D}$ is approximately between $2\widetilde{R} + 2$ and $4\widetilde{R} + 2$ (e.g., see curves for $\Xi = 40$ and $\widetilde{R} = 5.0$ in Fig. 6). This is the region wherein the counterions rearrange from a single layer in the midplane to two layers at the plates.

V. SUMMARY

In this manuscript we have presented a systematic investigation of the effect of counterion size on the interaction between two similarly charged plates. By computing the free energy as a function of the distance between the plates we have identified four interaction regimes depending on the size of the ions and electrostatic coupling constant. More specifically, we show that as the counterion size

is increased, the well known attraction between plates at high coupling regime can become repulsive. We show that the attractive contribution to the pressure from the electrostatic terms is a monotonically decreasing function of ion radius while the strength of the repulsive steric terms increases with ion radius. The latter starts to assert when the interaction parameter is greater than approximately (ip > 0.06), turning the interaction repulsive. We also observe that the finite ion size only affects the interaction for distances between the plates $2\widetilde{R} + 2 < \widetilde{D} < 4\widetilde{R} + 2$ which correspond to the ordering of ions from one to two layers.

Though the electric double layer has been extensively studied in the past, by theoretical and numerical simulation techniques, further theoretical work is required to better understand the contribution of the hard core on the interaction between similarly charged plates. To the best of our knowledge there are no reports on the calculation of the free energy of two interacting double layers. Here we have used a Wang–Landau approach to calculate the free energy of two interacting charged plates as a function of separation between them. The advantage of the Wang–Landau method over the use of the contact value theorem is in its extensibility to broader range of problems. Where the contact value theorem fails, a properly adjusted Wang–Landau MC simulations could step in.

[1] J. N. Israelachvili, *Intermolecular and Surface Forces* (Academic, London, 1991).
[2] Y. Levin, Rep. Prog. Phys. **65**, 1577 (2002).
[3] N. Ise, T. Konishi, and B. V. R. Tata, Langmuir **15**, 4176 (1999).
[4] K. Besteman, M. A. G. Zevenbergen, H. A. Heering, and S. G. Lemay, Phys. Rev. Lett. **93**, 170802 (2004).
[5] J. Urbanija *et al.*, Chem. Phys. Lipids **150/1**, 49 (2007).
[6] J. Urbanija *et al.*, Eur. Biophys. J. **37**, 1085 (2008).
[7] A. Moreira and R. R. Netz, Eur. Phys. J. E **8**, 33 (2002).
[8] H. Boroudjerdi *et al.*, Phys. Rep. **416**, 129 (2005).
[9] O. Punkkinen *et al.*, Europhys. Lett. **82**, 48001 (2008).

[10] B. E. Conway, Electrochim. Acta **40**, 1501 (1995).

[11] J. Cervera, J. A. Manzanares, and S. MafŽ, J. Membr. Sci. **191**, 179 (2001).

[12] E. Gouaux and R. MacKinnon, Science **310**, 1461 (2005).

[13] R. Kjellander and S. Marčelja, J. Phys. Chem. **90**, 1230 (1986).

[14] J. P. Valleau, R. Ivkov, and G. M. Torrie, J. Chem. Phys. **95**, 520 (1991).

[15] R. Kjellander, T. Akesson, B. Jönsson, and S. Marčelja, J. Chem. Phys. **97**, 1424 (1992).

[16] P. Bolhuis, T. Akesson, and B. Jönsson, J. Chem. Phys. **98**, 8096 (1993).

[17] V. Kralj-Iglič and A. Iglič, J. Phys. II **6**, 477 (1996).

[18] I. Borukhov, D. Andelman, and H. Orland, Phys. Rev. Lett. **79**, 435 (1997).

[19] C. N. Patra and S. K. Ghosh, J. Chem. Phys. **117**, 8938 (2002).

[20] M. Quesada-Pérez, A. Martín-Molina, and R. Hidalgo-Álvarez, J. Chem. Phys. **121**, 8618 (2004).

[21] D. Boda, D. Henderson, P. Plaschko, and W. R. Fawcett, Mol. Simul. **30**, 137 (2004).

[22] M. S. Kilic, M. Z. Bazant, and A. Ajdari, Phys. Rev. E **75**, 021502 (2007).

[23] J. G. Ibarra-Armenta, A. Martín-Molina, and M. Quesada-Pérez, Phys. Chem. Chem. Phys. **11**, 309 (2009).

[24] Y. Li and B.-Y. Ha, Phys. Rev. E **70**, 061503 (2004).

[25] D. Henderson, L. Blum, and J. L. Lebowitz, J. Electroanal. Chem. **102**, 315 (1979).

[26] H. Wennerstrom, B. Jönsson, and P. Linse, J. Chem. Phys. **76**, 4665 (1982).

[27] J. Lee, Phys. Rev. Lett. **71**, 211 (1993).

[28] F. Wang and D. Landau, Phys. Rev. E **64**, 056101 (2001).

[29] J. P. Hansen and I. R. McDonald, *Theory of Simple Liquids* (Academic, London, 1986).

[30] M. Schmidt and H. Löwen, Phys. Rev. Lett. **76**, 4552 (1996).

[31] J. Lekner, Physica A **176**, 485 (1991).

[32] R. Sperb, Mol. Simul. **20**, 179 (1998).

[33] F. Wang and D. P. Landau, Phys. Rev. E **64**, 056101 (2001).

[34] S.-H. Tsai, F. Wang, and D. P. Landau, Braz. J. Phys. **38**, 6 (2008).

[35] M. S. Shell, P. G. Debenedetti, and A. Z. Panagiotopoulos, Phys. Rev. E **66**, 056703 (2002).

[36] M. Troyer, S. Wessel, and F. Alet, Phys. Rev. Lett. **90**, 120201 (2003).

[37] E. B. Kim *et al.*, J. Chem. Phys. **117**, 7781 (2002).

[38] F. Calvo, Mol. Phys. **100**, 3421 (2002).

[39] N. Rathore, Q. Yan, and J. J. de Pablo, J. Chem. Phys. **120**, 5781 (2004).

[40] D. Frenkel and B. Smith, *Understanding Molecular Simulation* (Academic, San Diego, 1996).

[41] Q. Yan, T. S. Jain, and J. J. de Pablo, Phys. Rev. Lett. **92**, 235701 (2004).

[42] Though strictly not applicable to the present geometry the Carnahan–Starling equation of state, for volume fractions corresponding to $\widetilde{D} \sim 12$ also predicts that the hard sphere contribution to the pressure kicks in when the scaled radius is about four.

[43] A. Moreira and R. R. Netz, Phys. Rev. Lett. **87**, 078301 (2001).